

The (> Half) Empty Universe

Hagai El-Ad

*Racah Institute of Physics, The Hebrew University, Jerusalem, 91904
Israel*

Abstract. Voids are the most prominent feature of the large-scale structure of the universe. Still, they have been generally ignored in quantitative analysis of it, essentially due to the lack of an objective tool to identify the voids and to quantify them. To overcome this, we have developed the VOID FINDER algorithm, a novel tool for objectively quantifying voids in the galaxy distribution. We apply the algorithm to two redshift surveys, the dense SSRS2 and the full-sky *IRAS* 1.2 Jy. Both surveys show similar properties: $\sim 50\%$ of the volume is filled by the voids. The voids have a scale of at least $40 h^{-1}$ Mpc, and an average under-density of -0.9 . Faint galaxies do not fill the voids, but they do populate them more than bright ones. These results suggest that both optically and *IRAS* selected galaxies delineate the same large-scale structure. Comparison with the recovered mass distribution further suggests that the observed voids in the galaxy distribution correspond well to under-dense regions in the mass distribution. This confirms the gravitational origin of the voids.

1. Introduction

Perhaps one of the most intriguing findings of dense and complete nearby redshift surveys has been the discovery of large voids on scales of $\sim 50 h^{-1}$ Mpc, and that such large voids appear to be a common feature of the galaxy distribution. Early redshift surveys like the Coma/A1367 survey (Gregory & Thompson 1978) and the Hercules/A2199 survey (Chincarini *et al.* 1981) gave the first indications for the existence of voids, each revealing a void with a diameter of $\sim 20 h^{-1}$ Mpc. Surprising as these findings may have been, it was not before the discovery of the Boötes void (Kirshner *et al.* 1981) that the voids caught the attention of the astrophysical community (for a review, see Rood 1988).

The unexpectedly large void found in the Boötes constellation, confirmed to have a diameter of $\sim 60 h^{-1}$ Mpc (Kirshner *et al.* 1987), brought up the question whether the empty regions we observe are a regular feature of the distribution of galaxies, or rather rare exceptions. Wide-angle yet dense surveys, initially two-dimensional and more recently three-dimensional, probing relatively large volumes of the nearby universe, established that the voids are indeed a common feature of the large-scale structure (LSS) of the universe. The publication of the first slice from the CfA redshift survey (de Lapparent, Geller & Huchra 1986) introduced the picture of a universe where the galaxies are located on the surfaces of bubble-like structures, with diameters in the range $25\text{--}50 h^{-1}$ Mpc. The

extensions of the CfA survey (Geller & Huchra 1989), complemented in the south hemisphere by the SSRS and its extension, the SSRS2 (da Costa *et al.* 1988; 1994) have shown that not only large voids exist, but more importantly—that they occur frequently (at least judging by eye), suggesting a compact network of voids filling the entire volume.

The size of the structures observed in the redshift surveys is comparable to their effective depth. With voids as large as $60 h^{-1}$ Mpc in diameter (or perhaps even larger—see Broadhurst *et al.* 1990, and more recently Einasto *et al.* 1997), and walls extending over $\sim 100 h^{-1}$ Mpc, we might still not be seeing the full scope of the inhomogeneities in the distribution of galaxies, as we are limited by the surveys' dimensions. The largest survey available today, the *Las Campanas Redshift Survey* (LCRS) shows that structures on the scale of $100 h^{-1}$ Mpc are a common feature in the local ($z \leq 0.2$) universe (Landy *et al.* 1996). The LCRS, having an effective depth of $400 h^{-1}$ Mpc (if still only a two-dimensional survey), may thus suggest that we have reached the scale where the universe becomes homogeneous, as was speculated earlier (e.g., de Lapparent 1994). On the other hand, results from the shallower, though three-dimensional SSRS2 and CfA2 surveys (da Costa *et al.* 1994) indicate that we have not yet reached a fair sample. This question will be resolved only through the new generation of automated redshift surveys, like the *2-degree-Field* (2dF) survey (Lahav 1996) and the *Sloan Digital Sky Survey* (SDSS), expected to include up to 10^6 galaxies (Loveday 1996)—compared to today's $\sim 10^4$ galaxy surveys. These new surveys should be completed during the first decade of the next century.

It has been recognized early on that inhomogeneities on such scales could impose strong constraints on theoretical models for the formation of LSS. However, the voids have been largely ignored and their incorporation into theories of LSS has been relatively recent (Blumenthal *et al.* 1992; Dubinski *et al.* 1993; Piran *et al.* 1993). The major obstacle here has been the difficulty of developing proper tools to identify and to quantify them in an objective manner. As such, the description of a void-filled universe with a characteristic scale of $25\text{--}50 h^{-1}$ Mpc relied solely on the visual impression of redshift maps. In order to make a more quantitative analysis we have developed the VOID FINDER algorithm (El-Ad & Piran 1997) for the automatic detection of voids in three-dimensional surveys. Unlike other statistical measures, our target is to identify the *individual voids*, in as much the same way as voids are identified by eye. The main features of the algorithm are:

1. It is based on the point-distribution of galaxies, without introducing any smoothing scale which destroys the sharpness of the observed features.
2. It allows for the existence of some galaxies within the voids, recognizing that voids need not be completely empty.
3. It attempts to avoid the artificial connection between neighboring voids through small breaches in the walls, realizing that walls in the galaxy distribution need not be homogeneous as small-scale clustering will always be present.

After a review of some of the methods for analyzing the LSS (§2.), we describe the VOID FINDER algorithm (§3.) and the way it was tested using Voronoi

tessellations (§4.). We then apply the algorithm to the SSRS2 redshift survey (§5.) and to the *IRAS* 1.2 Jy (§6.). Finally (§7.), we discuss the results and summarize them.

2. Background

The various methods for describing the void content of the LSS of the universe can be divided into two categories: statistical measures, and algorithms for identifying individual voids within a sample. Additional *topological* measures, like the genus curve or percolation analysis, will not be discussed here.

The major statistical tool used for describing the voids is the *Void Probability Function* (VPF). It measures the probability $P_0(V)$ that a randomly positioned sphere of volume V contains no galaxies (White 1979). For a completely uncorrelated (Poissonian) distribution, it is $P_0(V) = \exp(-nV)$, where n is the number-density of galaxies, so that any departure from this quantity represents the signature for the presence of clustering. The major drawback of the VPF is that it is very sensitive to the details of the galaxy distribution. For instance, adding a few galaxies in the under-dense regions may greatly modify the VPF. A less sensitive variant of the VPF is the *Under-dense Probability Function* (UPF), defined as the probability $P_{\delta\rho/\rho}(V)$ that a randomly positioned sphere of volume V has a $\delta\rho/\rho$ under-density (Little & Weinberg 1994).

The first zero-crossing of the two-point correlation function $\xi(r)$ was used by Goldwirth *et al.* (1995) for determining the maximum diameters of voids in case of spherical voids. The two-point correlation function is defined as the probability in excess of Poisson distribution of finding a galaxy in a volume δV at a distance r away from a randomly chosen galaxy:

$$\delta P = n \delta V [1 + \xi(r)] \quad (1)$$

where n is the mean galaxy number-density. For a cellular like distribution the first-zero crossing is a direct measure of the characteristic size of the cells. Using Voronoi tessellations they show that despite the large uncertainty in the determination of $\xi(r)$ on large scales ($> 20 h^{-1}$ Mpc), the zero-crossing statistic may be a useful tool in determining the scale of typical voids—if the galaxy distribution is void-filled, and if there is a characteristic scale for the void distribution. Examining the SSRS2 sample, they found that $R_{\text{zero}} \approx 38 h^{-1}$ Mpc.

Previous works have used various definitions for voids, and applied different algorithms to identify them. Perhaps the first work identifying voids in a quantitative manner is that of Pellegrini *et al.* (1989), who examined ensembles of contiguous cells with densities below a given threshold. They use a cubic lattice, and define a local density for each cell in the lattice. This local density is based on the analysis of the smoothed density field. Groups of cells with densities below a specific limit constitute the voids. The algorithm considers two cells as contiguous if they are in contact either through their faces, edges or vertices. This technique was applied to the original SSRS, identifying 4 to 8 voids, depending on the density threshold. The major shortcomings of this algorithm are its use of a smoothed density field, and the lack of sense of the shape of the void it recognizes, allowing for practically any void shape.

Kauffmann & Fairall (1991) designed a more elaborate algorithm. They too used (empty) cubes, to which adjacent faces are attached. However, in order to avoid long finger-like extensions leading from one void into other voids, they impose a constraint on the adjacent faces, that each face must have an area of no less than two-thirds that of the surface on to which it is to be added. This scheme is restrictive, as it is tailored for finding only ellipsoidal-shaped voids. The algorithm was applied to the *Southern Redshifts Catalog* (SRC) and to an all-sky catalog, finding a peak in the spectrum of void diameters between 8 and $11 h^{-1}$ Mpc. This result is inconsistent with other estimates of the void sizes.

A more recent work applying another void search algorithm, is that of Lindner *et al.* (1995). In this work single spheres, that are devoid of a certain type of galaxies (depending on the morphological type and luminosity), are used. The algorithm was applied to an area north of the super-galactic (SG) plane, showing that voids defined by bright elliptical galaxies have a mean diameter of up to $40 h^{-1}$ Mpc, in agreement with the VOID FINDER results. When considering fainter galaxies, the voids are smaller, with the faintest galaxies studied defining $8 h^{-1}$ Mpc voids, suggesting that faint galaxies delineate smaller voids within larger ones, which are defined by the bright galaxies.

3. The VOID FINDER Algorithm

The VOID FINDER algorithm (El-Ad & Piran 1997) was designed with the following conceptual picture in mind: The main features of the LSS of the universe are voids surrounded by walls. The *walls* are generally thin, two-dimensional structures characterized by a high density of galaxies. They constitute boundaries between under-dense regions, generally ellipsoidal in shape—the *voids*. Although coherent over large scales, the walls—being subject to small-scale clustering—are not homogeneous and contain small breaches which we wish to ignore. Galaxies within walls are hereafter labeled *wall galaxies*, while the non-wall galaxies are named *field galaxies*. The voids are not totally empty: there are a few galaxies in them, which we call *void galaxies*.

We define a void as *a continuous volume that does not contain any wall galaxies, and is thicker than an adjustable limit*. In other words, one can freely move a sphere with the minimal diameter all through the void. This definition does not pre-determine the shape of the void: it can be a sphere, an ellipsoid, or have a more complex shape, including a non-convex one. The definition is targeted at identifying the same regions that would be recognized as voids, when interpreting a point distribution by eye. As the voids are defined based on the point distribution of galaxies, we do not need to introduce any smoothing scale. Our voids may contain galaxies. A stiffer requirement, such that voids should be completely empty, is too restrictive as a single galaxy located in the middle of what we would like to recognize as a void might prevent its identification. However, for this definition to be practical we must be able to identify the field galaxies before we can start locating the voids.

The algorithm is divided into two steps. First the WALL BUILDER identifies the wall galaxies and the field galaxies. Then the VOID FINDER locates the voids in the wall galaxy distribution. We define a wall galaxy as *a galaxy that has at least n other wall galaxies within a sphere of radius ℓ around it*. The radius ℓ is

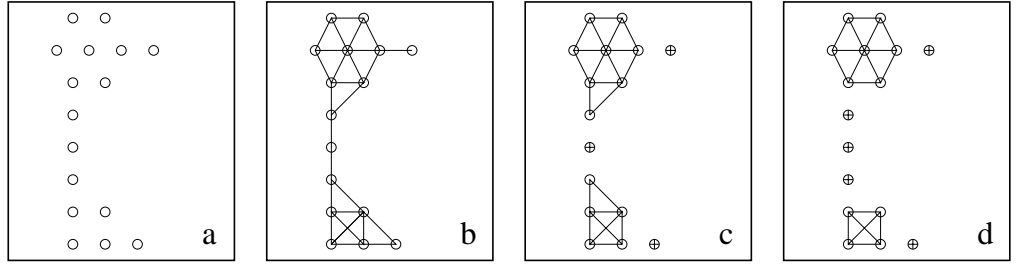


Figure 1. Wall construction using the WALL BUILDER. *Panel a*: A toy distribution of 16 galaxies (○). *Panel b*: After the calculation of ℓ , all galaxy pairs closer than this separation are marked. *Panel c*: Galaxies with less than three neighbors are flagged as field galaxies (⊕). *Panel d*: The final result: the string extending between the dense structures has been eliminated.

hereafter referred to as the *wall separation distance*. It is derived based on the statistics of the distance to the n 'th nearest neighbor. A galaxy that does not satisfy this definition is classified as a field galaxy. This is a recursive definition which we apply successively until all the galaxies are classified.

Fig. 1 demonstrates how the WALL BUILDER works for $n = 3$. Notice how the galaxy string is filtered, while the dense structures are identified and maintained. As a side-bonus of this procedure, originally dedicated to filtering the field galaxies, we obtain a visual identification of the walls. This is done by drawing all the links between wall galaxies satisfying $\text{dist}(\vec{x}_i, \vec{x}_j) < \ell$. These connections are not used in the next step of void analysis, but provide us with another visual tool to examine our results (e.g., see Fig. 3).

The VOID FINDER initially locates the voids containing the largest empty spheres. Following iterations locate the smaller voids, and—when appropriate—enlarge the volumes of the older voids. Spheres that are devoid of wall galaxies are used as building blocks for the voids. A single void is composed of as many superimposing spheres as required for covering all of its volume. The algorithm is iterative, with subsequent iterations searching for voids using a finer *void resolution*, defined as the diameter d_i of the minimal sphere used for encompassing a void during the i 'th iteration. The spheres for covering a void are picked up in two stages: the *identification stage*, followed by *consecutive enhancements*.

During the identification stage we locate the central parts of the void. Usually, these spheres cover only about half of the actual volume. We focus (at this stage) on identifying a certain void as a separate entity, rather than trying to capture all of its volume. The central parts of a void are covered using spheres with diameters in the range $\xi d_{\max} < d \leq d_{\max}$, with d_{\max} denoting the diameter of the void's largest sphere. The parameter ξ is the *thinness parameter*, which controls the flexibility allowed at this stage. Once a group of such intersecting spheres has been dubbed a void, it will not be merged with any other group. If the void is composed of more than one sphere (as is usually the case), then each sphere must intersect at least another one with a circle wider than the minimal diameter ξd_{\max} . We have taken $\xi = 0.85$, which allows for enough flexibility—still without accepting counter-intuitive void shapes.

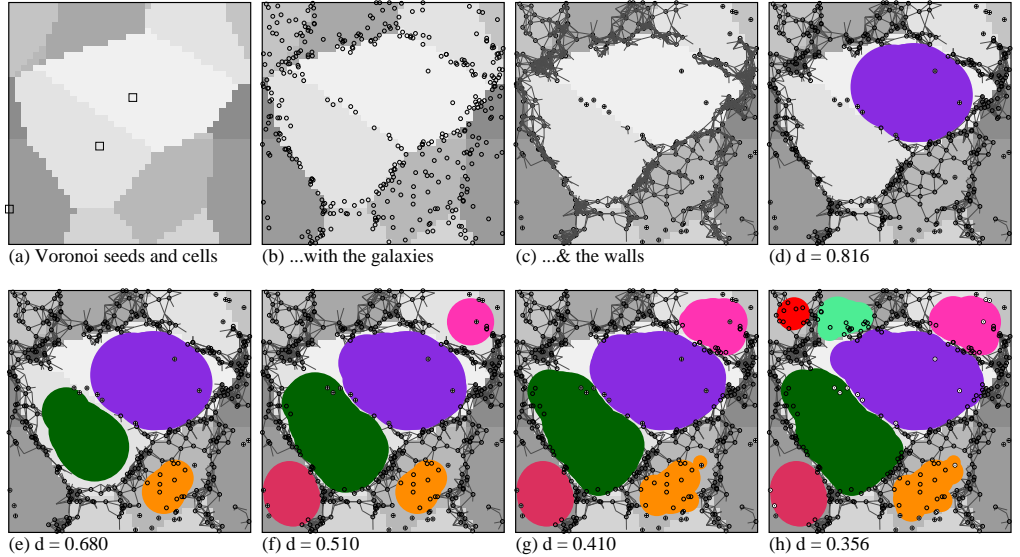


Figure 2. A demonstration of the way the VOID FINDER covers the voids. All panels depict the same slice, cut through a certain Voronoi tessellation. We present the Voronoi seeds (□) & cells (panel a), the galaxies (panel b) and the walls (panel c). The remaining panels show the voids' image, at various void resolutions d_i . More voids are recognized as we refine d_i , and the older voids are enlarged.

After the central part of a void is identified, we *consecutively enhance* its volume, in order to cover as much of the void volume as possible using the current void resolution. These additional spheres need not adhere to the ξ thinness limitation: we scan the immediate surroundings of each void, and if empty spheres are found then they are added to the void. We scan for enhancing spheres of a certain diameter only *after* scanning for new voids with that diameter. In this way we do not falsely break apart individual voids, and we do not prevent the identification of truly new voids (see Fig. 2).

To assess the statistical significance of the voids we compare the voids found in observed data with voids found in equivalent random distributions. The random distributions mimic the sample's geometry and density, and are analyzed by the algorithm in exactly the same manner. Averaging over the random catalogs we calculate $N_{\text{Poisson}}(d)$, the expected number of voids in a Poisson distribution as a function of the void resolution d . We compare this with the observed number, $N_{\text{survey}}(d)$. We define the *confidence level* as:

$$p(d) = 1 - \frac{N_{\text{Poisson}}(d)}{N_{\text{survey}}(d)} \quad (2)$$

The closer $p(d)$ is to unity, the less likely the void could appear in a random distribution. We consider voids with $p \geq 0.95$ as statistically significant. At a certain void resolution d_{stop} , $N_{\text{Poisson}}(d)$ exceeds $N_{\text{survey}}(d)$, and we terminate the void search.

The average galaxy number-density decreases with depth in a magnitude-limited redshift survey. If not corrected, this selection effect will interfere with the algorithm in the deeper regions of the sample: field galaxies will occur more frequently, and the derived size of the voids will be larger. Consequently, systematically larger voids will be found at greater distances. To avoid these effects, one should use a volume-limited sample, in which the galaxy number-density is constant and independent of the distance. A volume-limited sample with $M \leq M_o$ has a depth:

$$r_o = \sqrt{\mathcal{L}_o / 4\pi \mathcal{F}_{m_b}} = 10^{-5-0.2(M_o-m_b)} \text{ Mpc} \quad (3)$$

where m_b is the survey's magnitude limit and \mathcal{L}_o is the luminosity that corresponds to M_o . However, current volume-limited samples are too small to study the LSS. To overcome this, we use a semi-volume-limited sample: volume-limited up to some medium radius r_o , and magnitude-limited beyond. We choose the depth r_o by maximizing the number of bright galaxies $N(M \leq M_o)$:

$$N(M \leq M_o) = \frac{4\pi}{3} r_o^3 \cdot \eta \Gamma(1 - \alpha, x_o) \quad (4)$$

where η is the galaxy number-density. The incomplete Γ -function arises from the integration of the appropriate Schechter function (Schechter 1976), with $x = \mathcal{L}/\mathcal{L}_\star$.

No corrections are needed in the volume-limited region. We determine the values for ℓ and d_i in this region. Beyond r_o we define $\phi(r)$, a selection-function based on the Schechter luminosity-function:

$$\phi(r) = \frac{\Gamma(1 - \alpha, x_M)}{\Gamma(1 - \alpha, x_{M_o})} \quad (5)$$

where $x_M = 10^{-0.4(M-M_\star)}$. The selection-function $\phi(r)$ is the observed fraction of galaxies at the distance r , relative to r_o . Using $\phi(r)$ we modify both phases of the algorithm. In the WALL BUILDER phase, we scale the spheres' diameters by $\phi(r)$, thus considering larger spheres when counting neighbors at $r > r_o$. The same correction is applied to the VOID FINDER phase: A void of a given size found in a low density environment is less significant than a void of the same size found in a high density environment. In order that all the voids found in a given iteration are equally significant, we adjust the algorithm so that at a given iteration relatively larger voids are accepted, if located at $r > r_o$.

4. Voronoi Distributions

As a test-bed for the VOID FINDER algorithm, we use Voronoi distributions: A distribution of galaxies that is based on a Voronoi tessellation (Voronoi 1908). A Voronoi tessellation is a tiling of space into convex polyhedral cells, generated by a distribution of seeds. To generate a galaxy distribution in which the galaxies are located on the walls of the Voronoi cells, we have used an algorithm developed by Van de Weygaert & Icke (1989). The resultant galaxy distribution has the

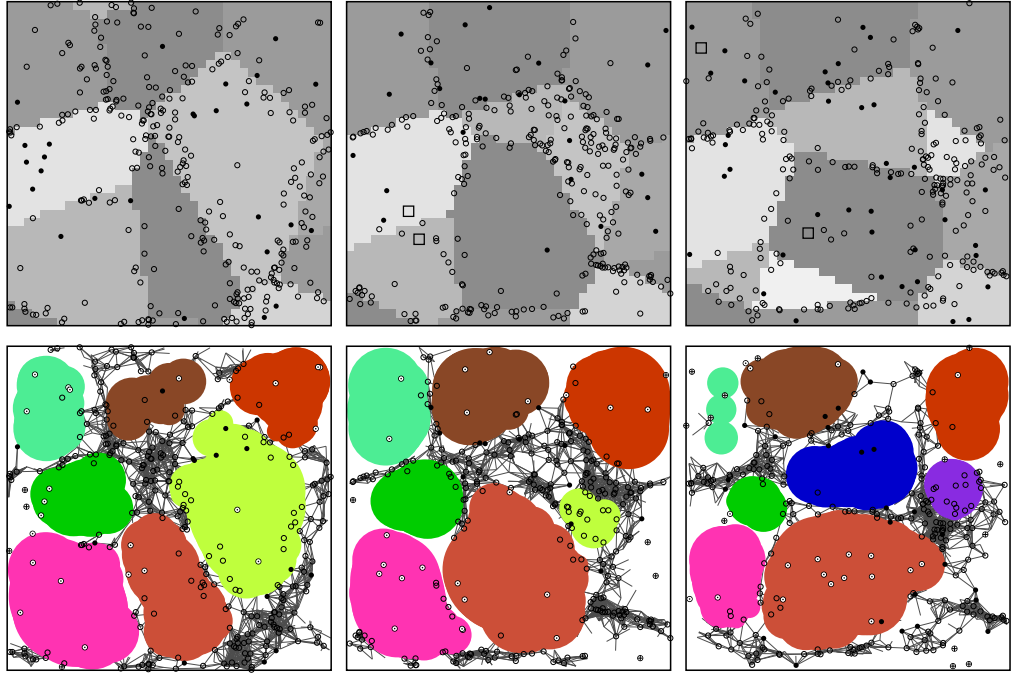


Figure 3. Three consecutive slices in a Voronoi tessellation, generated from 10 seeds with 3000 galaxies (10% random). *Upper row*: The Voronoi cells are depicted using gray shades, indicating the intersection of the cell with the central plane of the slab. Voronoi seeds are marked by ‘□’. Galaxies associated with cell boundaries are marked by ‘○’, and random galaxies by ‘●’. *Lower row*: The reconstructed voids. The voids are indicated using different colors, where the depicted voids correspond to the intersection of the central plane of each slab with the three-dimensional voids. Also shown are the walls (dark lines marking connections between nearby galaxies). Field galaxies, outside the voids, are marked by ‘⊕’, and void galaxies by ‘○’.

desired characteristic of large empty regions (i.e., voids), which we identify by the VOID FINDER algorithm.

A *Voronoi tessellation* is constructed from a given set of *seeds* $\{\vec{x}_i\}$. Based on the locations of these seeds, we divide the volume into cells. The Voronoi cell Π_i of seed i is defined by the following set of points \vec{x} :

$$\Pi_i = \{ \vec{x} \mid \text{dist}(\vec{x}, \vec{x}_i) < \text{dist}(\vec{x}, \vec{x}_j) \quad \text{for all } j \neq i \} \quad (6)$$

We assign a finite width to the walls and position the galaxies on the boundaries between the Voronoi cells, with a Gaussian displacement in the distance from the exact cell boundary. Additional random galaxies correspond to field galaxies. We will call a galaxy distribution constructed in this way a *Voronoi distribution*. The location and number of the Voronoi cells (the would-be voids), the spread of the wall galaxies and the fraction of random galaxies are all known. Therefore, we can use this distribution as a test bed for our algorithm.

We have constructed various Voronoi distributions and compared the original Voronoi tessellation to the VOID FINDER reconstruction (e.g., see Fig. 3). All Voronoi cells are reproduced except the very small cells near the boundaries, that are cut by the box limit. The reconstructed voids follow closely the original Voronoi cells, notwithstanding the noise introduced by the random galaxies. The walls highlighted using the WALL BUILDER are located along the boundaries between the Voronoi cells. We have also created mock surveys, based on Voronoi distributions. Galaxies in the Voronoi distribution were assigned magnitudes according to a Schechter function. Then, a magnitude-limited sample was chosen. To this Voronoi-based mock survey we have applied our usual procedure: analyzing a semi-volume-limited sample and applying corrections beyond r_o . The fit between the Voronoi cells and the recovered voids is still good, showing the adequacy of our method in analyzing actual surveys.

All together, the Voronoi tessellations that we examined show that the VOID FINDER indeed generates a faithful reproduction of the Voronoi cells. Further still, in cases where the reproduction merges adjacent Voronoi cells into one void, we see this as the adequate outcome of a missing wall. If we would have examined such a galaxy distribution by eye, with no prior knowledge about the locations of the Voronoi cells, we too would most likely consider that volume—originally occupied by two Voronoi cells—as one void. A level of $\sim 10\%$ random galaxies is tolerated, with no significant distortion in the void reproduction, and Voronoi-based mock surveys are also reproduced faithfully.

5. The SSRS2 sample

The SSRS2 survey (da Costa *et al.* 1994) consists of ~ 3600 galaxies with $m_b \leq 15.5$ in the region $-40^\circ < \delta < -2.5^\circ$ and $b \leq -40^\circ$, covering 1.13sr . We have considered a semi-volume-limited sample, in this case consisting of galaxies brighter than $M_o \leq -19$, corresponding to a depth $r_o = 79.5 h^{-1} \text{Mpc}$. The Schechter luminosity function was evaluated with $M_\star = -19.5$ and $\alpha = 1.2$, as derived for the SSRS2. Our final semi-volume-limited sample consists of 1898 galaxies, extending out to $r_{\max} = 130 h^{-1} \text{Mpc}$ where the selection-function ϕ has dropped to 17%. It should be emphasized that the SSRS2 analysis is performed in *redshift-space*. However, because of the paucity of large clusters and the small amplitude of peculiar motions in the volume surveyed by the SSRS2, redshift distortions are small (da Costa *et al.* 1997) and the properties derived here should reflect those of voids in real-space.

The WALL BUILDER analysis of the SSRS2 has classified 91.5% of the galaxies as wall galaxies, and 8.5% as field galaxies. The wall separation distance was $\ell = 7.4 h^{-1} \text{Mpc}$. In the volume-limited region we have $n^{-1/3} = 6.4 h^{-1} \text{Mpc}$, so $\ell/n^{-1/3} = 1.16$. The wall galaxies are grouped in ten structures: one structure contains most (96%) of the wall galaxies. The rest of the wall galaxies are found in nine groups, each having 4 to 21 galaxies.

We have identified eleven significant ($p \geq 0.95$) voids within the volume probed by the SSRS2. These voids were detected while the void resolution was $d \geq 19.2 h^{-1} \text{Mpc}$. In the following calculations we take into account only these voids, unless otherwise specified. Seven additional voids were identified before the void search was terminated at the resolution $d_{\text{stop}} = 15.1 h^{-1} \text{Mpc}$, for which

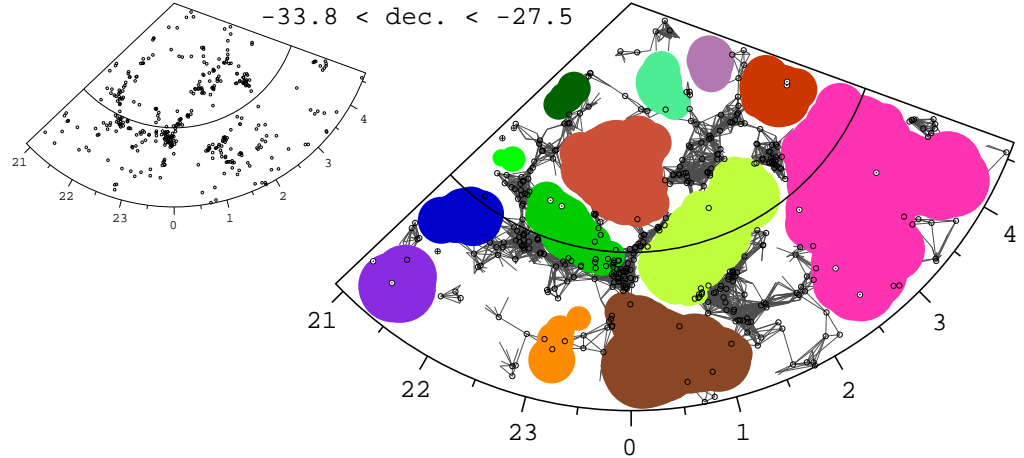


Figure 4. A slice through the SSRS2 sample (*left*) and the resultant VOID FINDER reconstruction (*right*). The slice contains many voids, walls and filaments. The outstanding structure from ($\alpha = 4^h$, $r = 45 h^{-1} \text{ Mpc}$) to ($\alpha = 0^h$, $r = 90 h^{-1} \text{ Mpc}$) is the Southern Wall (SW). The Pavo-Indus-Telescopium (PIT) supercluster runs along the line of sight at $\alpha = 21^h.5$.

p vanishes. Initial results for the SSRS2 were reported in El-Ad, Piran & da Costa (1996). The locations and characteristics of all eighteen voids are given in Table 1 of El-Ad & Piran (1997).

The average size of the voids in the SSRS2 as estimated from the equivalent diameters is $\bar{d} = 40 \pm 12 h^{-1} \text{ Mpc}$. The average under-density within the voids was found to be $\delta\rho/\rho \approx -0.9$, a quite remarkable result showing how empty voids are of bright galaxies. The eleven significant voids comprise 54% of the survey's volume. An additional 5% is covered by the seven additional voids, totaling in $\sim 60\%$ of the volume being occupied by these voids. We estimate that the walls occupy less than 25% of the volume. A single $6^{\circ}25$ -wide constant-declination slice through the SSRS2 is presented in Fig. 4.

The largest void found in the SSRS2 survey has an equivalent diameter $d = 60.8 h^{-1} \text{ Mpc}$, making it comparable in volume to the large void found in the Boötes (Kirshner *et al.* 1981). This void is an ellipsoid, whose major axis is perpendicular to the line of sight, located at: $80 h^{-1} \text{ Mpc} < r < 130 h^{-1} \text{ Mpc}$; $-25^\circ < \delta < -2.5^\circ$; $21^h < \alpha < 23^h.75$. This void might actually be larger, since it is bounded (in three directions) by the limits of the SSRS2. A second large void (with $d = 56.2 h^{-1} \text{ Mpc}$) is also comparable to the Boötes void.

When preparing the semi-volume-limited sample, we cast off all faint $M > M_o$ galaxies in the region $r < r_o$. These galaxies comprise the bulk of the surveyed galaxy population that we are forced to ignore (the rest are $r > r_{\max}$ galaxies, where the sample is too sparse). Although we cannot use these galaxies during the analysis phases, we can still try and benefit from them *a posteriori*: after the voids are located, we examine the locations of these galaxies. Almost 61% of the $r < r_o$ region is covered by voids—but only 19% of the 1264 faint galaxies are found within them. Even though the VOID FINDER algorithm uses

only the brighter galaxies in this region, we find that the faint galaxies do not fill the voids, providing an excellent verification of the algorithm. Still, the percentage of faint galaxies within the voids is significantly larger than that of the bright galaxies: only $\sim 5\%$ of the bright $M_o \leq -19$ galaxies are contained in the voids.

6. The *IRAS* sample

The *IRAS* survey contains 5321 galaxies complete to a flux limit of 1.2 Jy (Fisher *et al.* 1995). We applied corrections for the computed peculiar velocities, to obtain the real-space distribution of the galaxies. In the void analysis, we have limited ourselves to galaxies extending out to $r_{\max} = 80 h^{-1}$ Mpc, and created a semi-volume-limited sample with a depth $r_o = 50 h^{-1}$ Mpc. The selection function drops to 22% at r_{\max} . The final sample consists of 1876 galaxies, and 1531 faint galaxies were eliminated in order to create the volume-limited region.

The sky coverage of the *IRAS* is almost complete (87.6%), with the galactic plane region $|b| < 5^\circ$ constituting most of the excluded zones. Various schemes (e.g., Yahil *et al.* 1991) have been used to extrapolate the density field to the galactic plane, but these are not directly applicable to our analysis. Thus, when looking for voids we avoid the ZOA, treating it as a rigid boundary practically cutting the *IRAS* to two halves. Since the ZOA cuts across voids this scheme divides some voids to two and eliminates others. However, it is the most conservative method, and therefore the results for the volumes of the voids should be considered as lower limits. We estimate the effect of this method by examining the opposite approach in which the ZOA is treated as if it is a part of the survey, applying no corrections. The ZOA is nowhere wider than the minimal void resolution used, so it does not create new voids by itself. Therefore the effect of including the ZOA is to overestimate the size of voids near it, because it allows the merging of a couple of voids and the expansion of other voids into the region. Still the overall effect on the void statistics is limited.

The WALL BUILDER analysis of the *IRAS* galaxy distribution located 95% of the galaxies within walls. We find that the walls occupy at most $\sim 25\%$ of the examined volume. This corresponds to an average wall over-density of at least $\delta\rho/\rho \approx 4$. Since the *IRAS* sample is relatively sparse, we have considered all the galaxies while identifying the voids. Hence, the *IRAS* voids presented below are *completely empty*.

Applying our most conservative approach to analyze the *IRAS*—i.e., including the field galaxies and avoiding the ZOA—we have identified 24 voids of which twelve are statistically significant at a 0.95 confidence level (El-Ad, Piran & da Costa 1997). In general, some of the voids we find are smaller than their actual size—because of the way we treat the ZOA, or because the field galaxies were not removed from the analysis. Both effects imply that our estimates of the size of voids are likely to be lower limits.

In the SG plane (Fig. 5, panel *a*) one recognizes void 10 as the Sculptor Void (da Costa *et al.* 1988), located below the P-I-T part ($Y < 0$) of the Great Attractor (GA), seen here to be composed of several sub-structures. Adjacent to it we find void 1, stretching parallel to the Cetus wall. These two voids are separated only by a few field galaxies. If we filter them out, the two would

merge to form one huge void, equivalent in volume to a $d = 62 h^{-1}$ Mpc sphere occupying most of that part of the skies. Voids 1 & 10 are limited by the r_{\max} boundary of our sample, so they could prove to be larger still.

The area above the Perseus-Pisces (PP) supercluster (up to the Great Wall near Coma, at $Y = 70 h^{-1}$ Mpc) is occupied by two voids: 7 & 11. If the field galaxies are filtered first, these two voids merge. Also note in this area the minor void ($p = 0.21$) located below the Coma supercluster, at $(X = -7, Y = 54)$: this void corresponds to the largest void found in the CfA survey (de Lapparent, Geller & Huchra 1986). The closest void we found (void 14), can be seen in the center of this panel, just below the local supercluster. Another clear, and rather nearby, void in the SG plane is void 15, in front of PP. A minor void can be viewed beyond the $Y > 0$ section of the GA, at $(X = -51, Y = 19)$.

The average size of the twelve significant *IRAS* voids as estimated from the equivalent diameters is $\bar{d} = 40 \pm 6 h^{-1}$ Mpc. The increase in average void diameter in the *IRAS* compared to the SSRS2 ($\sim 5\%$) is due to the relatively narrow angular limits of the latter survey. The twelve most significant *IRAS* voids occupy 22% of the examined volume; considering all 24 voids, the volume is 32%. If we consider only the volume-limited region of our sample, where there are no distortions caused by the survey's r_{\max} boundary (only the ZOA), the void volume reaches 46%. We have also examined the void distribution in redshift-space. As expected, voids in redshift-space are typically bigger than their real-space counterparts. The total void volume in redshift-space is $\sim 20\%$ larger than that in real-space, and the average diameter of the significant voids in redshift-space is $44 h^{-1}$ Mpc (compare Fig. 5, panel *a*, with Fig. 6, right panel).

After the voids were located we examined the locations of the previously eliminated faint galaxies. Only 13% of these are located within the voids, in agreement with the identification of the voids based on the brighter galaxies. However, as found in the SSRS2, there is a notable increase in the number of faint galaxies in the voids, compared to the number of brighter galaxies.

What is the effect of the limitations we have imposed in our void analysis? As stated above, the treatment of the ZOA as a rigid boundary and the consideration of only empty voids, cause us to interpret the results derived in this way as a lower limit. An upper limit is derived by taking the opposite approach, this time including the ZOA and filtering the field galaxies. Each factor alone corresponds to an increase in the average void diameter of 5–15%. Together the effect is $\sim 20\%$, yielding an upper limit for this sample of $\bar{d} = 48 h^{-1}$ Mpc. A similar increase occurs in the total void volume. When filtering the field galaxies the voids are not empty, now having an average under-density of $\delta\rho/\rho \approx -0.9$, as found for the SSRS2.

7. Discussion

We have used the VOID FINDER algorithm to analyze two redshift surveys: The SSRS2 and the *IRAS* 1.2 Jy. These surveys represent two extreme cases in the trade-off between density and sky coverage. The SSRS2 is densely sampled ($m_b \leq 15.5$), but it has narrow angular limits, especially in the declination range. As a result, voids are often limited by the survey's boundary, diminishing their scale. The *IRAS* is an almost full-sky survey (87.6% coverage), but it is

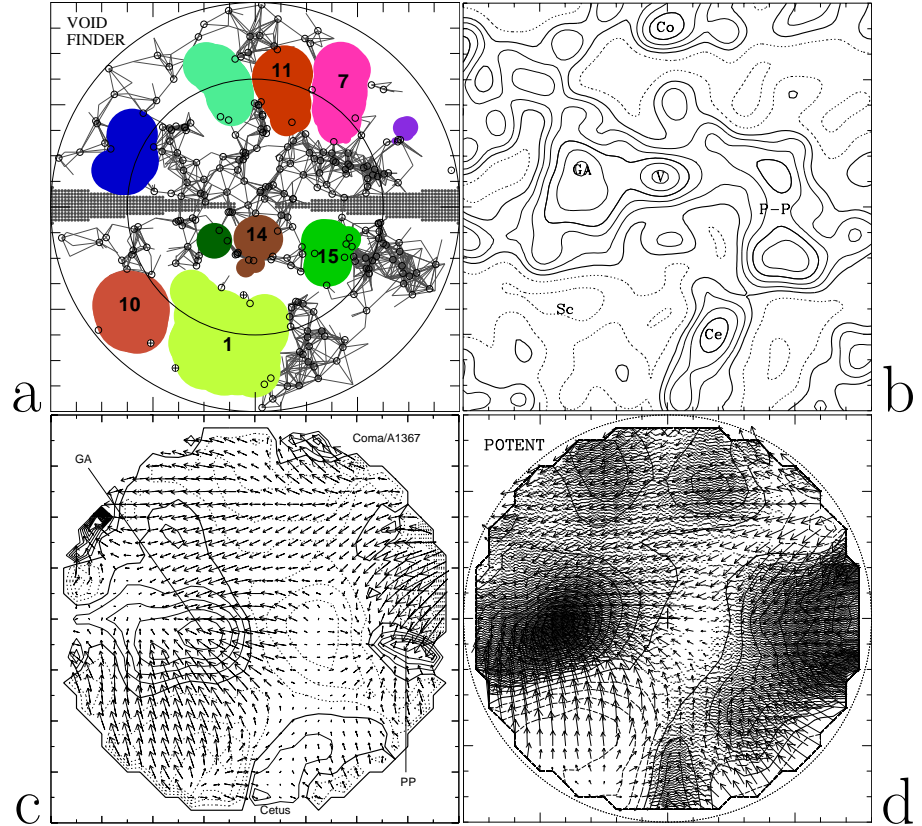


Figure 5. The supergalactic plane extending out to $80 h^{-1}$ Mpc, as depicted by various techniques. *Panel a* (El-Ad, Piran & da Costa 1997): The real-space locations of the voids and the walls in the *IRAS* 1.2 Jy sample, using the VOID FINDER algorithm. The excluded ZOA is indicated along $Y = 0$. The depicted galaxies extend $5 h^{-1}$ Mpc above and below the plane. Wall galaxies are marked as by ‘o’, field galaxies by ‘⊕’. All the galaxies are located outside the voids—galaxies that seem to be in a void appear so due to the two-dimensional projection. The inner circle at $r_o = 50 h^{-1}$ Mpc marks the volume-limited region of our sample. *Panel b* (Strauss & Willick 1995): The real-space smoothed density field of *IRAS* galaxies, using $5 h^{-1}$ Mpc Gaussian smoothing, extrapolating into the ZOA. The density field is obtained by a self-consistent correction for peculiar velocities with $\beta = 1$. Reproduced by permission of Michael Strauss. *Panel c* (da Costa *et al.* 1996): The reconstructed velocity and density fields obtained from the SFI sample, using $9 h^{-1}$ Mpc Gaussian smoothing. The arrows give the X – Y components of the three-dimensional velocity field. The contours are of δ , spaced at 0.2 intervals. The heavy solid line indicates $\delta = 0$. Reproduced by permission of Luiz da Costa. *Panel d* (Dekel 1994; Dekel *et al.* 1997): The smoothed velocity field and the resultant density field as recovered by POTENT from the Mark III data, using $12 h^{-1}$ Mpc Gaussian smoothing. Reproduced by permission of Avishai Dekel.

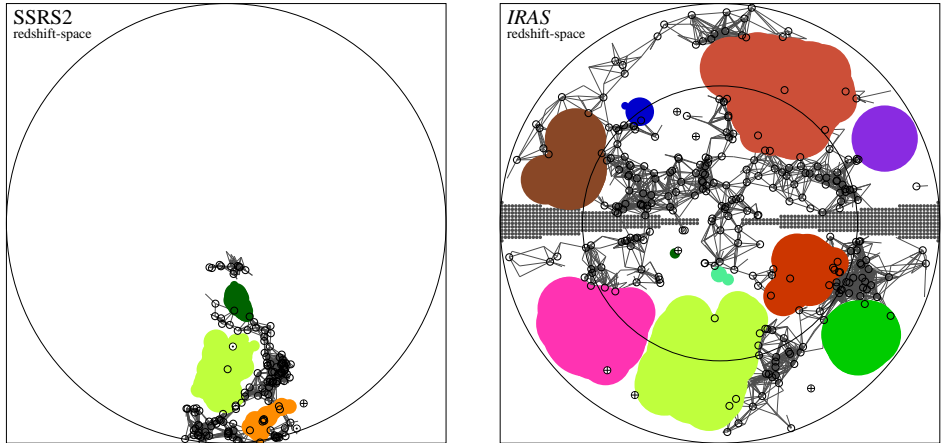


Figure 6. Redshift-space voids in the SG plane: SSRS2 (*left*) and *IRAS* (*right*). The denser sampling of the SSRS2 is evident. Similar voids are found in the overlapping regions of the surveys. For the *IRAS*, compare also the real- and redshift-space distribution: the *IRAS* voids in redshift-space are larger, and the dense structures appear much more collapsed, than in real-space (Fig. 5, panel *a*).

rather sparse. As a result one cannot use a small void resolution, for lack of statistical significance. In addition to the above differences, the SSRS2 galaxies are optically selected, as opposed to the *IRAS* galaxies.

Withstanding these differences, the results obtained with these surveys are similar. First, the surveys agree regarding individual voids in the regions where the surveys overlap. Fig. 6 depicts the redshift-space voids in the SG plane, for the *IRAS* and for the corresponding part of the SSRS2. In the region where the SSRS2 sample overlaps the *IRAS* sample, we find three of the eleven significant voids identified in the SSRS2. The corresponding *IRAS* voids are $\sim 33\%$ larger than the SSRS2 ones, since they are not bounded by narrow angular limits as the SSRS2 voids.

Additionally, the results agree *viz a viz* the voids' statistical characteristics:

1. Large voids occupy $\sim 50\%$ of the volume.
2. Walls occupy less than $\sim 25\%$ of the volume.
3. A void scale of at least $40 h^{-1} \text{ Mpc}$, with an average under-density of -0.9 .
4. Faint galaxies do not fill the voids, but they do populate them more than bright ones.

The void scale derived in both surveys is a lower limit: for the SSRS2, because of the narrow boundaries limiting the voids; and for the *IRAS*, due to the larger d_{stop} , and because of the conservative analysis applied regarding the ZOA and the field galaxies.

The fact that both the *IRAS* and the SSRS2 are consistent regarding the void statistics as well as the individual voids is not trivial, since the *IRAS*

galaxies represent a special galaxy class, possibly biased relative to the optical galaxies (Lahav, Rowan-Robinson & Lynden-Bell 1988). The agreement between the surveys suggests that a similar void scale exists for both optically and *IRAS* selected galaxies. This suggests that the voids are also devoid of dark matter, indicating that they have formed gravitationally (Piran *et al.* 1993).

The *IRAS* data also provides a suitable benchmark as it has been used to derive the smooth density field, and it probes a volume comparable to that used to determine the density field of the underlying mass distribution from the POTENT reconstruction method (Dekel, Bertschinger & Faber 1990), based on the measured galaxy peculiar velocity field (see Fig. 5). The voids and walls identified by the VOID FINDER indeed correspond to the under- and over-dense regions in the *IRAS* density field (Strauss & Willick 1995) respectively. Comparison with the SFI sample (da Costa *et al.* 1996) also demonstrates that the voids delineated by galaxies correspond remarkably well with the under-dense regions in the reconstructed mass density field derived from peculiar velocities (but see also the Mark III map—Dekel 1994; Dekel *et al.* 1997). This confirms the idea suggested earlier, that the observed voids in redshift surveys represent true voids in the mass distribution, forcing a gravitational theory for their formation.

Most of the over-dense regions, walls and filaments, are narrower than $10 h^{-1}$ Mpc. The smoothing scale used for creating the density fields spreads the originally thin structures over wider regions, extending into the under-dense volumes. This has the effect of giving a false impression of a rather blurred galaxy distribution, where prominent over-dense structures are separated by small under-dense regions. The true picture is very different: there is a sharp contrast between the thin over-dense structures which occupy only the lesser part of the volume, and the large voids. The notion of a void filled universe cannot be avoided in this picture.

We have developed and tested a new tool for quantifying the large-scale structure of the universe. Unlike most of the work in this field, we focus on the under-dense regions, and for the first time are capable of individually identifying and statistically quantifying the voids. The VOID FINDER analysis clearly shows the prominence of the voids in the LSS, not hindered by smoothing of the over-dense regions, and it reveals the image of a void-filled universe, where large voids are a common feature.

The consistency in the void image between *IRAS* and optically selected galaxies suggests that galaxies of different types delineate equally well the observed voids. Therefore galaxy biasing is an unlikely mechanism for explaining the observed voids in redshift surveys. Comparison with the recovered mass distribution further suggests that the observed voids in the galaxy distribution correspond well to under-dense regions in the mass distribution. This confirms the gravitational origin of the voids.

Acknowledgments. I am indebted to Tsvi Piran for his guidance and encouragement throughout this research. I would like to warmly thank Luiz da Costa for providing the SSRS2 data and for numerous helpful discussions. I am grateful to Avishai Dekel and Michael Strauss, for providing two of the figures, and to Rien Van de Weygaert for providing his Voronoi tessellation code. I am happy to acknowledge the support of the Israeli MFA and of the Casa96 organizing committee.

References

Blumenthal, G. R., da Costa, L. N., Goldwirth, D. S., Lecar, M., & Piran, T. 1992, The largest possible voids, *ApJ*, 388, 234

Broadhurst, T. J., Ellis, R. S., Koo, D. C., & Szalay, A. S., 1990, Large-scale distribution of galaxies at the galactic poles, *Nature*, 343, 726

Chincarini, G., Rood, H. J., & Thompson, L. A. 1981, Supercluster bridge between groups of galaxy clusters, *ApJ*, 249, L47

da Costa, L. N., *et al.* 1988, The southern sky redshift survey, *ApJ*, 327, 544

da Costa, L. N., *et al.* 1994, A complete southern sky redshift survey, *ApJ*, 424, L1

da Costa, L. N., Freudling, W., Wegner, G., Giovanelli, R., Haynes, M. P., & Salzer, J. J. 1996, The mass distribution in the nearby universe, *ApJ*, 468, L5 ([astro-ph/9606144](#))

da Costa, L. N., *et al.* 1997, in preparation

de Lapparent, V. 1994, Mapping the large-scale structure, in *Astronomy from Wide-Field Imaging*, eds. H. T. MacGillivray *et al.* (IAU), p. 669

de Lapparent, V., Geller, M. J., & Huchra, J. P. 1986, A slice of the universe, *ApJ*, 302, L1

Dekel, A., Bertschinger, E., & Faber, S. M. 1990, Potential, velocity, and density fields from sparse and noisy redshift-distance samples - Method, *ApJ*, 364, 349

Dekel, A. 1994, Dynamics of cosmic flows, *ARA&A*, 32, 371

Dekel, A., Eldar, A., Kolatt, T., Yahil, A., Willick, J. A., Faber, S. M., Corteau, S., & Burstein, D. 1997, in preparation

Dubinski, J., da Costa, L. N., Goldwirth, D. S., Lecar, M., & Piran, T. 1993, Void evolution and the large-scale structure, *ApJ*, 410, 458

Einasto, J., *et al.* 1997, A 120-Mpc Periodicity in the Three-Dimensional Distribution of Galaxy Superclusters, *Nature*, 385, 139 ([astro-ph/9701018](#))

El-Ad, H., Piran, T., & da Costa, L. N. 1996, Automated detection of voids in redshift surveys, *ApJ*, 462, L13 ([astro-ph/9512070](#))

El-Ad, H., Piran, T., & da Costa, L. N. 1997, A catalogue of the voids in the *IRAS* 1.2 Jy survey, *MNRAS*, in press ([astro-ph/9608022](#))

El-Ad, H., & Piran, T. 1997, Voids in the large-scale structure, *ApJ*, accepted ([astro-ph/9702135](#))

Fisher, K. B., Huchra, J. P., Strauss, M. A., Davis, M., Yahil, A., & Schlegel, D. 1995, The *IRAS* 1.2 Jy survey: Redshift data, *ApJS*, 100, 69 ([astro-ph/9502101](#))

Geller, M. J., & Huchra, J. P. 1989, Mapping the universe, *Science*, 246, 897

Goldwirth, D. S., da Costa, L. N., & Van de Weygaert, R. 1995, The two-point correlation function and the size of voids, *MNRAS*, 275, 1185 ([astro-ph/9503002](#))

Gregory, S. A., & Thompson, L. A. 1978, The Coma/A1367 supercluster and its environs, *ApJ*, 222, 784

Kauffmann, G., & Fairall, A. P. 1991, Voids in the distribution of galaxies: an assessment of their significance and derivation of a void spectrum, *MNRAS*, 248, 313

Kirshner, R. P., Oemler, A. Jr., Schechter, P. L., & Shectman, S. A. 1981, A million cubic megaparsec void in Boötes?, *ApJ*, 248, L57

Kirshner, R. P., Oemler, A. Jr., Schechter, P. L., & Shectman, S. A. 1987, A survey of the Boötes void, *ApJ*, 314, 493

Lahav, O., Rowan-Robinson, M., & Lynden-Bell, D. 1988, The peculiar acceleration of the Local Group as deduced from the optical and IRAS flux dipoles, *MNRAS*, 234, 677

Lahav, O. 1996, Present and future galaxy redshift surveys: ORS, DOGS and 2dF, in proceedings *Mapping, Measuring and Modeling the Universe*, Valencia, September 1995, eds. P. Coles & V. Martinez, APS ([astro-ph/9601054](#))

Landy, S. D., Shectman, S. A., Lin, H., Kirshner, R. P., Oemler, A. A., & Tucker, D. 1996, The 2D power spectrum of the Las Campanas redshift survey: Detection of excess power on $100h^{-1}\text{Mpc}$ scales, *ApJ*, 456, L1 ([astro-ph/9510146](#))

Lindner, U., Einasto, J., Einasto, M., Freudling, W., Fricke, K., & Tago, E. 1995, The structure of supervoids – I: Void hierarchy in the northern local supervoid, *A&A*, 301, 329 ([astro-ph/9503044](#))

Little, B., & Weinberg, D. 1994, Cosmic voids and biased galaxy formation, *MNRAS*, 267, 605 ([astro-ph/9306006](#))

Loveday, J. 1996, The Sloan digital sky survey: status and prospects, talk given at the *XXXIst Rencontres de Moriond*, Les Arcs, Savoie, France, January 1996 ([astro-ph/9605028](#))

Pellegrini, P. S., da Costa, L. N., & de Carvalho, R. R. 1989, Voids in the southern galactic cap, *ApJ*, 339, 595

Piran, T., Lecar, M., Goldwirth, D. S., da Costa, L. N., & Blumenthal, G. R. 1993, Limits on the Primordial Fluctuation Spectrum: Void Sizes and Anisotropy of the CMBR, *MNRAS*, 265, 681 ([astro-ph/9305019](#))

Rood, H. J. 1988, Voids, *ARA&A*, 26, 245

Schechter, P. 1976, An analytic expression for the luminosity function of galaxies, *ApJ*, 203, 297

Strauss, M. A., & Willick., J. A. 1995, The density and peculiar velocity fields of nearby galaxies, *Phys. Rep.*, 261, 271 ([astro-ph/9502079](#))

White, S. D. M. 1979, The hierarchy of correlation functions and its relation to other measures of galaxy clustering, *MNRAS*, 186, 145

Van de Weygaert, R., & Icke, V. 1989, Fragmenting the universe. II - Voronoi vertices as Abell clusters, *A&A*, 213, 1

Yahil, A., Strauss, M. A., Davis, M., & Huchra, J. P. 1991, A redshift survey of *IRAS* galaxies. II. Methods for determining self-consistent velocity and density fields, *ApJ*, 372, 380

Voronoi, G. 1908, Nouvelles applications des paramètres continus à la théorie des formes quadratiques. Deuxième Mémoire - Recherches sur les paralléloèdres primitifs, *J. reine angew. Math.*, 134, 198